Impact of gravitational force on facial skin sagging across age groups using a custom-built imaging device: Evidence from French women

Remo Campiche*[1], Marie Cherel[2], Ghislain François[2], Charlotte Peucat[2], Florian Cocogne[3], Etienne Camel[3], Bernhard Fink[4, 5], Peter Kollias[6], Mathias Gempeler[1], Rainer Voegeli[1]

[1]Beauty & Care, dsm-firmenich, Kaiseraugst, Switzerland, [2]QIMA Newtone SAS, Qima Life Sciences, [3]Institut d'Expertise Clinique (IEC), Lyon, France, [4]Department of Evolutionary Anthropology, University of Vienna, Vienna, [5]Biosocial Science Information, Biedermannsdorf, Austria, [6]Canfield Scientific Europe, Utrecht, Netherlands

1. Introduction

Wrinkles and skin sagging of the face correlate positively with chronological age [1] and are key indicators of perceived age across ethnic groups [2-4]. Sagging is characterized by the loss of skin elasticity and firmness, caused by degradation of the extracellular matrix, particularly elastic fibres and collagen network [5, 6], and a loss in subcutaneous adipose mass [7]. Visible signs of facial skin sagging include the nasolabial folds, marionette lines, and jaw sagging. Age-related skin displacements occur due to the gravitational force pulling the skin downward. The severity of sagging can be graded by photonumeric scales [8]. Additionally, various devices have been developed to quantify skin elasticity and firmness. A commonly used device is the Cutometer®, which uses a vacuum to draw the skin into an aperture. The amplitude of skin displacement and the skin's ability to return to its original position after strain indicate elasticity and firmness. DynaSKIN is a non-contact device that projects an airstream perpendicularly onto the skin, causing an indentation that measures skin firmness [9]. Moreover, three-dimensional (3D) methodologies and reviscometer® have been employed to evaluate the directionality of skin displacements under the influence of gravity [10,11]. Finally, research has conducted photographic analyses to compare skin sagging between subjects in vertical (upright) versus horizontal (supine) positions [12].

We present a new methodology for evaluating the impact of gravity on facial skin across the entire face and specific regions. A robust, custom-made device, consisting of a motorized, adjustable chair that can be moved from vertical to horizontal positions at various angles, was constructed. This movement simulates the effect of gravitational force in different directions while capturing a participant's face in 3D and 2D. A proof-of-concept study evaluated the device's precision in measuring facial skin displacements and thus sagging severity across five age cohorts and positions, simulating different gravitational forces.

2. Materials and Methods

2.1. Custom-built imaging device

Our device consists of a metal frame construction with a fixed frame standing on the ground. A participant can be comfortably seated on a rotating chair. Attached to the metal construction is a motorized rotating frame allowing the rotation of the participant's body for facial image acquisition in various positions, from vertical (upright) to horizontal (supine). A 3D Vectra system (Canfield Scientific Inc., USA) and a 2D high-resolution Nikon D5600 (Nikon Corp., Japan) camera equipped with a 40 mm lens are attached to the rotating frame in front of a seat (Fig. 1). An additional lateral camera uEye XS (Imaging Development Systems GmbH, Germany) monitors the position of the participant. Flashes are integrated into the Vectra system for 3D-acquisition. Dedicated flashes are used for frontal 2D images. The seat contains a styrofoam headrest. The seat is also motorized in height for initial positioning of the participant, and adjustment during the rotation. Custom-made software was developed for 3D and 2D image acquisition and the system rotation (QIMA Newtone SAS, France). The software includes a reposition/correction module for slight movements of subjects during position changes.
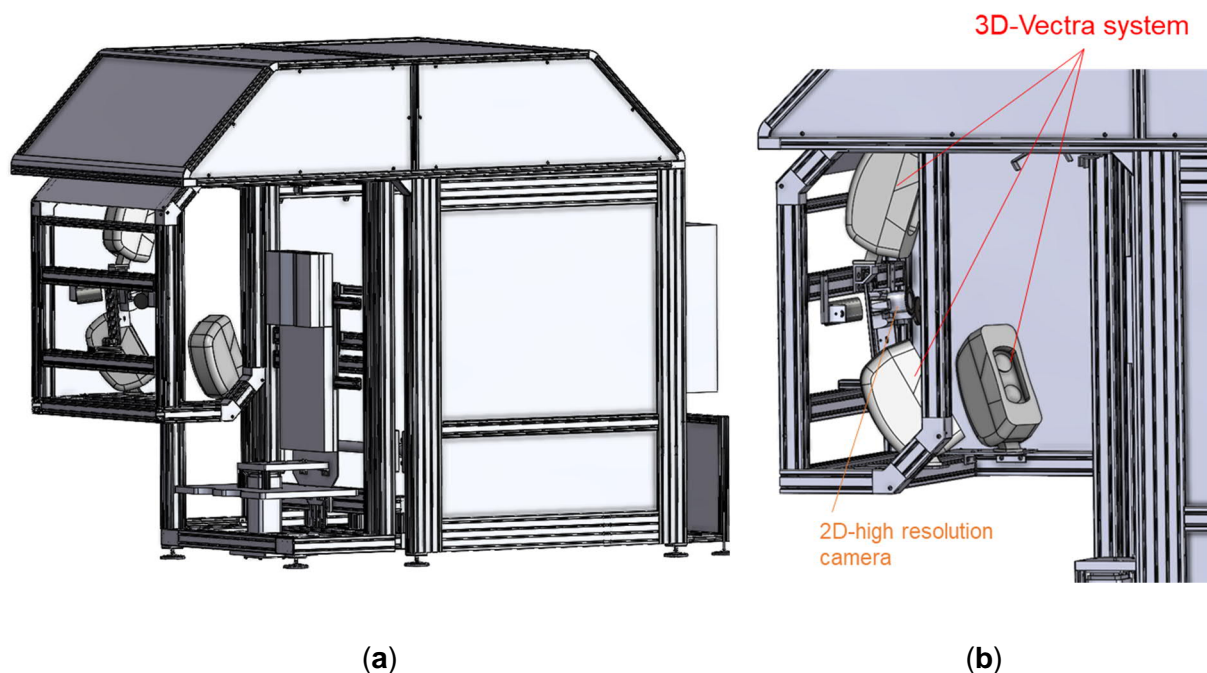

(**a**)   (**b**)

Figure 1. (a) Scheme of the 3D imaging device with a motorized chair in upright (vertical) position. (b) Close-up of the camera systems in the device.

2.2. Proof-of-concept study

This proof-of-concept study was conducted between 26th November and 4th December 2024 in Lyon, France. Female volunteers visited the laboratory once for measurements and were acclimatized for 20 minutes in an air-conditioned room at 21±2 °C and 50±10% relative humidity. They wore a black cap to cover their hair and a tank top to make the neckline visible. This study was performed in compliance with the Standard Operating Procedures of the Institut d'Expertise Clinique and according to the principles of Good Clinical Practices published by I.C.H. (Topic E6(R2): EMA/CHMP/ICH/135/1995).

There was a washout phase of 24 hours before coming to the laboratory. No cosmetic or pharmaceutical products were allowed on the face and the neck/neckline, except for a neutral cleanser.

2.3. Study panel

60 Caucasian women (Fitzpatrick skin phototype II to IV, aged 20 – 69 years) living in the Lyon area of France were recruited. The participants were distributed in five age groups with n=12 each and an age difference between groups of 10±2 years (Table 1).

Table 1. Study panel age groups.

Age group [years]	Mean age [years]
20-29	24.8
30-39	35.0
40-49	45.6
50-59	55.8
60-69	64.8
All	45.2

2.4. Measurement of skin displacements

Participants were comfortably seated in the device with a relaxed, neutral facial expression. The head rested on a firm styrofoam block with a triangular cutout to keep the head in place during chair movements. 3D and 2D images were taken at angles 0° (upright, "baseline"), 22.5°, 45°, 67.5°, 90° (horizontal, supine) with closed eyes. Slight head movements during participant and camera movements were adjusted to the Frankfurt horizontal plane (Fig. 2a) and fixed reference areas on the forehead and the nose tip that were considered not to move with changes of gravitational force (Fig. 2b).
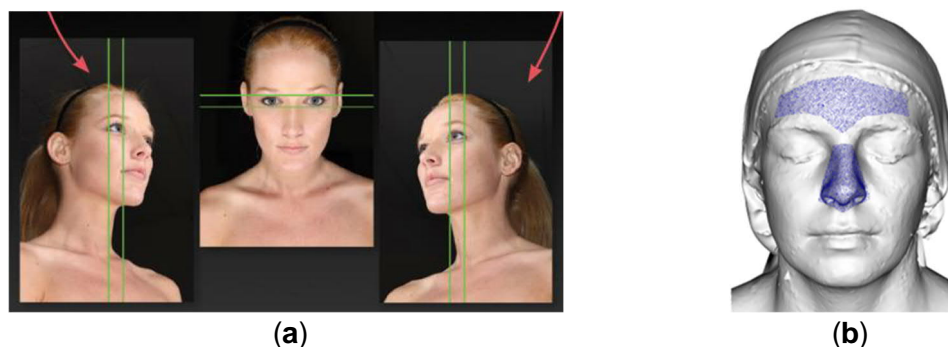

(**a**)   (**b**)

Figure 2. Position check before image acquisition and fixed reference areas 3D-alignment in vertical position. (a) 2D images and eye alignment for correct participant positioning; (b) Reference areas on the forehead and the nose (in blue) provide the baseline planes.

Skin displacements were calculated in x-, y-, and z-directions from the 3D images relative to the baseline position (0°). Three regions of interest (ROIs) were chosen for separate analysis, i.e., the under-eye region, the nasolabial folds, and the cheeks (Fig. 3). Cheek sagging impacts nasolabial fold formation, which is a major visible sagging sign [13]. The under-eye area was included because of the known age-related impact of gravity and volume descent [14]. Two types of spatial representation of the movements (here called 'maps') were generated. *Distance maps* are front face maps showing the distance of the skin to the baseline surface at different positions (of the participant) using a colour gradient. *Deformation maps* show the directional displacement of the skin with vectors.

Skin displacements were assessed separately for each half of the face. The three directions of movement were combined into a single, positive deformation vector (mean deformation amplitude).
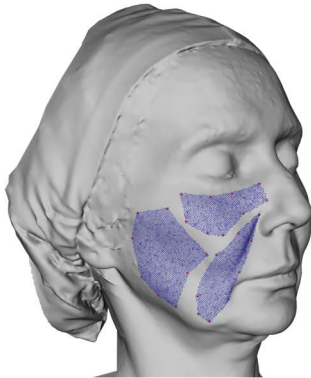

Figure 3. Visualization of the three ROIs chosen for analysis of the skin displacements.

2.5. Statistics
Group comparisons (participants' positions, or age-groups) were performed using ANOVA models with post-hoc Tukey tests for pairwise comparisons. Significance threshold was set to p=0.05. Pearson correlations (r) were performed to assess the relationship between participants' age and the skin deformations. Minitab software was used for all statistical tests.

3. Results

3.1. Facial skin displacements increased significantly with increasing position angle
We calculated the mean normalized direction of the skin movement for each ROI. For all three regions, we found a clear increase in facial displacements with increasing angle (under-eye: F=303.9, p<0.001; cheek: F=530.04, p<0.001; nasolabial fold: F=420.3; p<0.001; all three ROI combined: F=443.34, p<0.001) (Fig. 4). Pairwise post-hoc comparisons showed omnibus statistically significant differences between the position angles (Table 2).
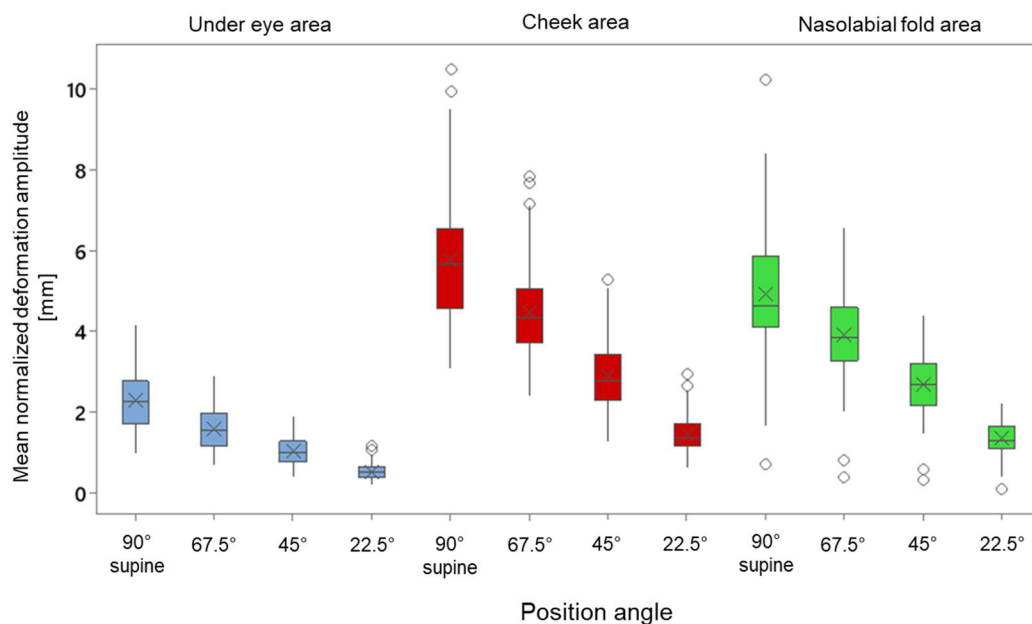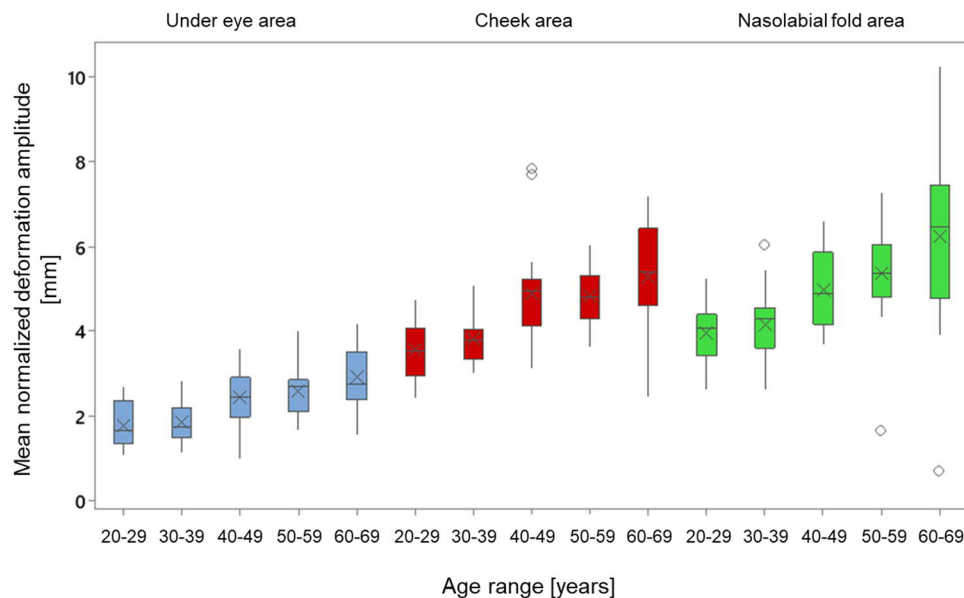

Figure 4. Facial skin deformation amplitude on the three facial regions of interest increased significantly with increasing position angle.

Table 2. Post-hoc pairwise comparisons between position angles for skin deformation amplitude. *NS* = not significant, *S* = significant.

ROI	Under eye area			Cheek area			Nasolabial fold area		
Position angle	67.5°	45°	22.5°	67.5°	45°	22.5°	67.5°	45°	22.5°
90°	S	S	S	S	S	S	S	S	S
67.5°		S	S		S	S		S	S
45°			S			S			S

3.2. Facial skin displacements increased with age

We found a clear increase in facial displacements with the age of the volunteers at each ROI (under-eye: F=17.0, $p<0.001$; cheek F=16.11, $p<0.001$; nasolabial fold: F=15.09, $p<0.001$; all three ROI combined: F=52.56, $p<0.001$) (Fig. 5). Pairwise post-hoc comparisons showed indicated multiple statistically significant differences between the age groups (Table 3).

Figure 5. Age-dependent facial skin deformation amplitude for the three regions of interest at the 90° angle (supine position). The deformation amplitude increased with age.

Table 3. Post-hoc pairwise comparisons between age groups for skin deformation amplitude at 90° supine position. *NS* = not significant, *S* = significant.

ROI, position angle	Under eye area, 90° (supine)				Cheek area, 90° (supine)				Nasolabial fold area, 90° (supine)			
Age group	30-39 yrs	40-49 yrs	50-59 yrs	60-69 yrs	30-39 yrs	40-49 yrs	50-59 yrs	60-69 yrs	30-39 yrs	40-49 yrs	50-59 yrs	60-69 yrs
20-29 yrs	NS	S	S	S	NS	S	S	S	NS	S	S	S
30-39 yrs		S	S	S		S	S	S		NS	S	S
40-49 yrs			NS	S			NS	NS			NS	S
50-59 yrs				NS				NS				NS

The pattern of the results in Figure 5 and Table 3 at the 90° supine position suggested that the major change in skin sagging happens at around 40-49 years, indicated by the increase in deformation amplitude seen in each ROI. This is confirmed by calculating all ROI (full face) deformations against the three greatest position angles 45°, 67.5° and 90° (F=38.16, p<0.001) (Fig. 6). This is also supported by pairwise post-hoc comparison indicating significant differences between the 30-39 and the 40-49 year age groups becoming evident athe 67.5° and the 90° position angle (Table 4).
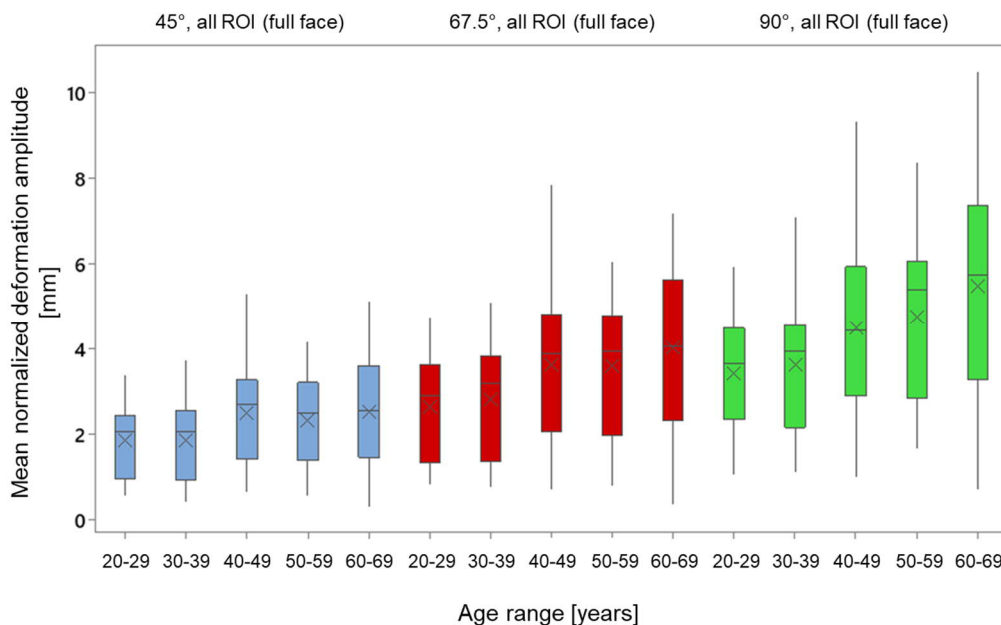

Figure 6. Age-dependent facial skin deformation amplitude for the three ROIs combined (full face) at the greatest position angles. The deformation amplitude increased with age and position angle.

Table 4. Post-hoc pairwise comparisons between age groups for skin deformation amplitude at the three greatest position angles. *NS* = not significant, *S* = significant

Position angle	45° (full face)				67.5° (full face)				90° (supine, full face)			
Age group	30-39 yrs	40-49 yrs	50-59 yrs	60-69 yrs	30-39 yrs	40-49 yrs	50-59 yrs	60-69 yrs	30-39 yrs	40-49 yrs	50-59 yrs	60-69 yrs
20-29 yrs	NS	NS	NS	NS	NS	S	S	S	NS	S	S	S
30-39 yrs		NS	NS	NS		S	S	S		S	S	S
40-49 yrs			NS	NS			NS	NS			S	S
50-59 yrs				NS				NS				NS

3.3. Correlation of deformation amplitude with volunteer age

We plotted the mean normalized deformation amplitude on the three ROIs versus the age of the volunteers. This yielded a moderate but significant correlation between amplitude and age for all ROIs (Fig. 7).
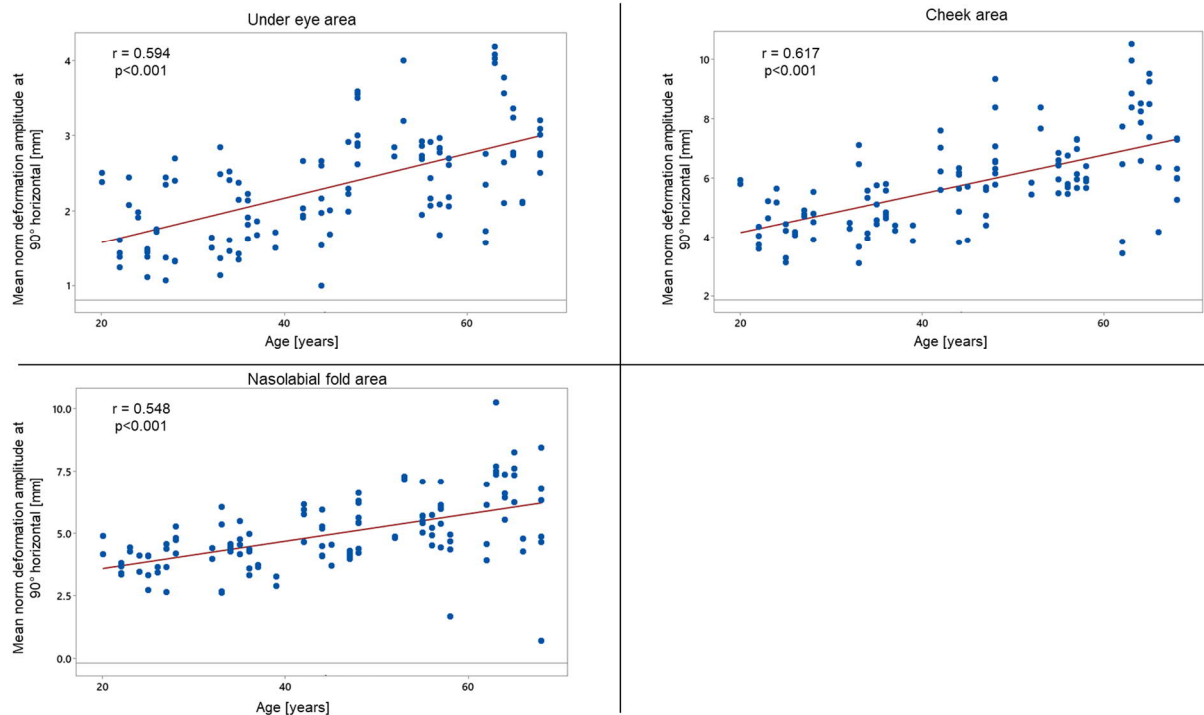
Figure 7. Relationship between normalized deformation amplitude and the age of volunteers for the three regions of interest in supine position. The red line represents the linear regression (under eyes: r^2=0.35; cheek: r^2=0.38; nasolabial fold: r^2=0.30).

3.4. Distance maps of volunteers showed distinct displacements between different positions and age groups.

Gravity-dependent distance changes were mapped on facial images using a colour gradient to provide comprehensive and tangible illustrations of position-dependent skin deformation amplitudes. The 3D images were used to create distance maps for the whole face. A gradient from white to blue visualized the distance increase relative to the 0° vertical position. A gradient from white to orange was used to visualize the distance decrease relative to the vertical position. The resulting facial colour maps indicate the magnitude of facial displacement during position changes (Fig. 8). Blue colour intensity around the nasolabial fold area and the cheek increased with the participant's position/angle. Due to gravity, the skin was pulled backwards, i.e., away from the baseline plane. The increase in blue colour was more pronounced in the older subject than in the younger one, indicating a greater displacement. The 2D images show a smoothing of the facial features towards the horizontal position, which was more pronounced for the older versus the younger volunteer (Fig. 8).

3.5. Deformation maps showed directional movements of facial skin dependent on position angle and age group.

We calculated 3D vectors and visualized the direction of movement across the face. This resulted in 3D facial scans featuring arrows indicating the direction and magnitude of the movement (Fig. 9). The number and intensity of the arrows increased with increasing position/angle and were lower in younger than in older volunteers. Furthermore, the directionality of the arrows changed with position angle and thus gravity.
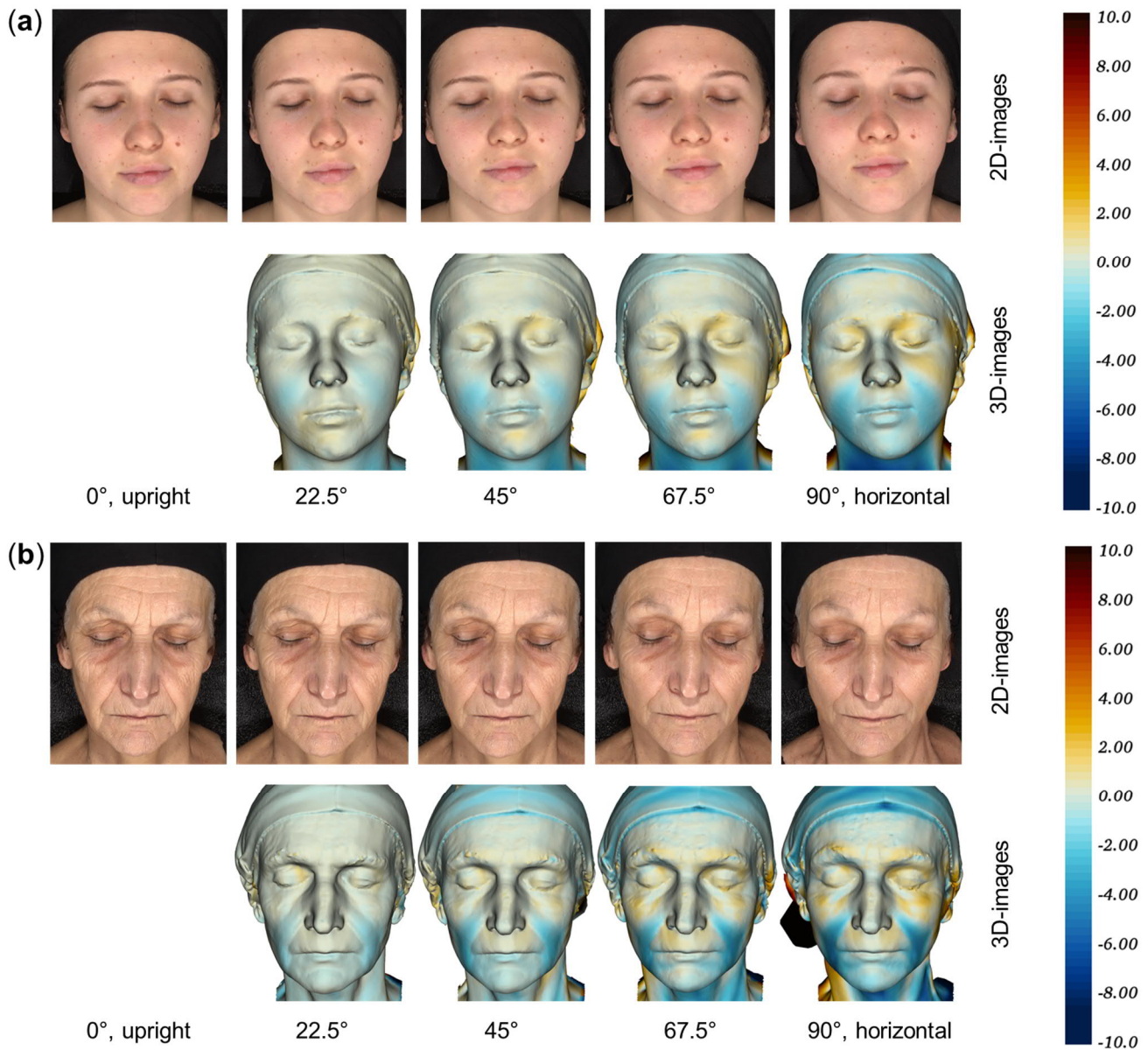
Figure 8. High-resolution 2D images and 3D head scans with distance maps of a selected 22-year-old (a) and a 65-year-old volunteer (b) at the different positions. Distances towards 0° (vertical position) are shown as a blue-to-red gradient on the bars at the right. Blue areas indicate deformation backwards due to directional changes in gravity at the different positions.

4. Discussion

We present an innovative approach to studying age-related facial skin sagging. Skin sagging was assessed by measuring skin displacements at different levels of gravity using a custom-built device (Fig. 1). Facial images were acquired at distinct positions, and skin displacements were computed for the full face. Our approach builds on 3D facial colour mapping technology 15] and extends previous assessments of skin deformation in 3D for every pixel of a facial photograph or 3D head scan (Figs. 8 and 9). In the present observational proof-of-concept study, we document quantifyable differences in skin displacements of three disting regions of interest (under-eye, cheek, nasolabial fold) in French women depending on gravitational force (Fig. 4).
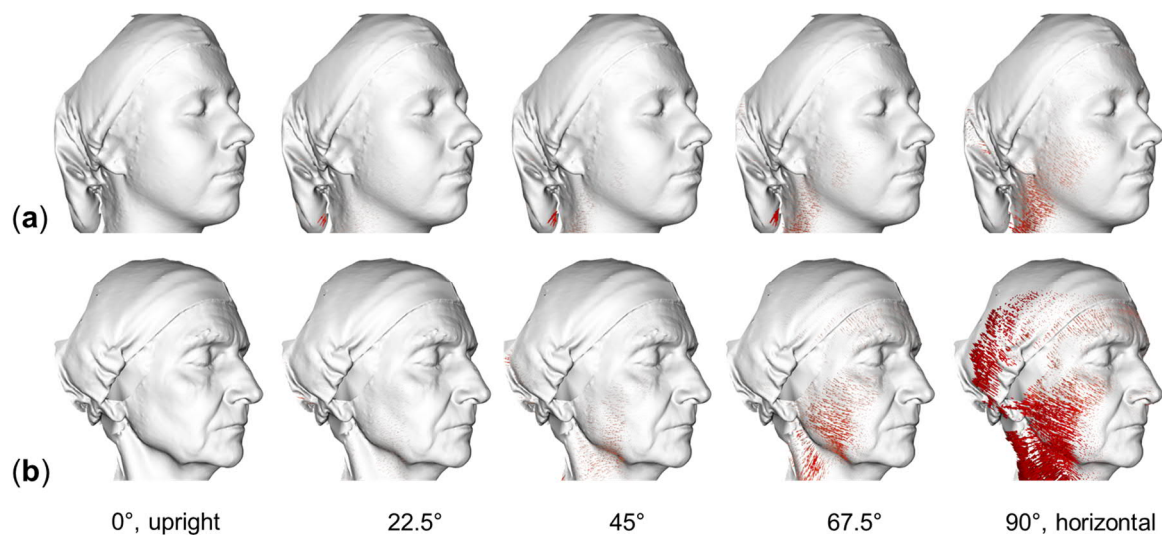
| 0°, upright | 22.5° | 45° | 67.5° | 90°, horizontal |

Figure 9. Deformation maps of directional skin displacements as arrows for a selected 22-year-old volunteer (a) and a 65-year-old volunteer (b) at the different positions.

Specifically, we found good resolution in terms of skin deformation with increasing participants' position/angles from upright to supine position (Fig. 4). Considering age-dependent differences, facial skin movements measured as mean deformation amplitude increased in the older age groups (Figs. 5 and 7) and participants' age correlated positively with deformation amplitude (Fig. 7). The results in Figure 5 and Table 3 suggested that all three ROI behaved similarly with regards to deformation at the differen position angles and with regards to age albeit the magnitude of the deformation amplitude increased with age or position angle. Interestingly, there seems to be a significant change at around 40-49 years of age (Fig. 5). This was confirmed by comparing all three ROI combined (full face) for age range versus the three greatest position angles (Fig. 6). Again, a significant change at around the age of 40-49 was found for all three positions. This may suggest a critical age window concerning facial aging and thus anti-aging interventions.

Given the significant separation of the directional skin deformations found with our new device, we propose that our methodology has enough resolution for applications in cosmetic science, treatment, and business-related concerns. In addition, our findings suggest an important threshold for the aging face around life's midpoint.

5. Conclusion

We constructed a device to measure facial skin displacements depending on gravitational force. Age-related skin deformations were examined in French women. The results indicate differences in skin deformations that could be quantified, mapped, and visualized for interpretation. The current methodology presents a powerful, comprehensive, and user-friendly way to assess facial skin sagging, ready for use and application in dermatology and cosmetic science.

6. References

1.　Tsukahara, K., et al., *Determination of age-related changes in the morphological structure (sagging) of the human cheek using a photonumeric scale and three-dimensional surface parameters.* Int J Cosmet Sci, 2000. **22**: p. 247-258.

2.　Voegeli, R., et al., *Predictors of female age, health and attractiveness perception from skin feature analysis of digital portraits in five ethnic groups.* Int J Cosmet Sci, 2023. **45**(5): p. 672-687.

3.　Fink, B., et al., *Self Versus Third party Perceptions of Female Age, Health and Attractiveness.* Cosmetics & Toiletries, 2024. **139**(3): p. 38-DM32.

4.　Flament, F., A. Abric, and A.S. Adam, *Evaluating the respective weights of some facial signs on perceived ages in differently aged women of five ethnic origins.* J Cosmet Dermatol, 2021. **20**(3): p. 842-853.

5.　Imokawa, G. and K. Ishida, *Biological mechanisms underlying the ultraviolet radiation-induced formation of skin wrinkling and sagging I: reduced skin elasticity, highly associated with enhanced dermal elastase activity, triggers wrinkling and sagging.* Int J Mol Sci, 2015. **16**(4): p. 7753-75.

6.　Imokawa, G., H. Nakajima, and K. Ishida, *Biological mechanisms underlying the ultraviolet radiation-induced formation of skin wrinkling and sagging II: over-expression of neprilysin plays an essential role.* Int J Mol Sci, 2015. **16**(4): p. 7776-95.

7.　Ezure, T. and S. Amano, *Influence of subcutaneous adipose tissue mass on dermal elasticity and sagging severity in lower cheek.* Skin Res Technol, 2010. **16**(3): p. 332-8.

8.　Ezure, T., et al., *Sagging of the cheek is related to skin elasticity, fat mass and mimetic muscle function.* Skin Res Technol, 2009. **15**(3): p. 299-305.

9.　Kearney, E.M., et al., *Evaluation of skin firmness by the DynaSKIN, a novel non-contact compression device, and its use in revealing the efficacy of a skincare regimen featuring a novel anti-ageing ingredient, acetyl aspartic acid.* Skin Res Technol, 2017. **23**(2): p. 155-168.

10.　Saito, N., et al., *Development of a new evaluation method for cheek sagging using a Moire 3D analysis system.* Skin Res Technol, 2008. **14**(3): p. 287-92.

11.　Ohshima, H., et al., *Relevance of the directionality of skin elasticity to aging and sagging of the face.* Skin Res Technol, 2011. **17**(1): p. 101-7.

12.　Flament, F., R. Bazin, and B. Piot, *Influence of gravity upon some facial signs.* Int J Cosmet Sci, 2015. **37**(3): p. 291-7.

13.　Ezure, T. and S. Amano, *Involvement of upper cheek sagging in nasolabial fold formation.* Skin Res Technol, 2012. **18**(3): p. 259-64.

14.　Mally, P., C.N. Czyz, and A.E. Wulc, *The Role of Gravity in Periorbital and Midfacial Aging.* Aesthet Surg J, 2014. **34**(6): p. 809-22.

15.　Voegeli, R., et al., *Facial skin mapping: from single point bio-instrumental evaluation to continuous visualization of skin hydration, barrier function, skin surface pH, and sebum in different ethnic skin types.* Int J Cosmet Sci, 2019. **41**: p. 411-424.